Engineering Metal-Organic Frameworks for the Electrochemical Reduction of CO_2: A Mini-review

Riming Wang,[a] Freek Kapteijn,[a] and Jorge Gascon*[a,b]

Abstract: Electrochemical CO_2 reduction holds great promise in reducing atmospheric CO_2 concentration. However, several challenges hinder the commercialization of this technology. Energy efficiency, CO_2 solubility in aqueous phase, and electrode stability are among the current issues. In this mini-review, we summarize and highlight the main advantages and limitations that Metal-Organic Frameworks may offer to this field of research, either when used directly as electrocatalysts or when used as catalyst precursors.

1. Introduction

The ever-increasing atmospheric CO_2 concentration is one of the critical issues that require an urgent solution within this century. From a global carbon cycle point of view, industrial activity is the major CO_2 contributor, causing a rapid accumulation of this greenhouse gas in the atmosphere. To counteract this unbalance, CO_2 capture and utilization technologies should be implemented. In this spirit, several technologies have been proposed for CO_2 utilization, based on thermocatalysis, photocatalysis, and electrocatalysis, *etc*. All the above-mentioned catalytic approaches have their economic advantages under certain conditions, and they may all contribute to reducing atmospheric CO_2.[1] For example, thermocatalysis would already be economically competitive if green H_2 (*e.g.* generated from water splitting using renewable energy) was massively available.[2] Photocatalysis, on the other hand, would be more favorable in remote locations with strong solar irradiation. Electrocatalytic reduction of CO_2 (CO_2ER) is the other technology that holds great promise if efficient electrocatalysts can be developed for the direct transformation of CO_2 into valuable products.

Initially, catalysts used for CO_2ER were pure metal foils directly used as electrodes.[3] With the advancement of nanotechnology, other configurations have been used as catalysts in CO_2ER, significantly enhancing CO_2ER efficiency.[4] In these nanostructured electrocatalysts, the active phase is dispersed within a conductive support, such as carbon cloth, carbon paper or glassy carbon. In the following context, the electrode mainly refers to catalysts dispersed on a conductive support, and catalyst engineering represents the engineering effort to improve CO_2ER efficiencies (including Faradaic efficiencies toward valuable products, current densities, and energy efficiencies) through the design of catalytic sites and/or the optimization of the catalyst structure.

Metal-organic frameworks (MOFs) have recently emerged in the field of catalysis because of their unique textural and topological properties.[5] On the one hand, when MOFs are used directly as catalysts, not only the atomically dispersed metal nodes can be engineered into active sites, but also the organic linkers hold great potential as catalytic sites.[6] Besides, the porous structure can be tuned to enhance mass transport. On the other hand, MOFs can also be used as catalyst precursors, yielding MOF mediated catalysts.[7] Following this approach, the MOF is decomposed under controlled conditions to lead to the clustering of its metal component into small nanoparticles or to the formation of single atom catalytic sites. At the same time, the organic component (the linker) rearranges into a carbonaceous matrix that may be conductive.[8] Xia *et al*. reviewed the use of MOFs for electrochemical energy storage, including catalytic electrodes.[9] Herein, we summarize the recent works on electrochemical CO_2 reduction using MOF and MOF derived catalysts.

Next to reviewing the work done so far on this interesting topic, we have to realize that the commercialization of CO_2ER will not solely rely on catalyst engineering. Indeed, the design of the electrochemical cell and the optimization of reaction conditions (pressure, temperature, *etc.*) will play a role as important as that of the catalyst itself.

In this mini-review, we first give a brief introduction to the challenges faced by CO_2ER, followed by a summary on MOF-related catalyst engineering and MOF derived electrocatalysts. We finalize with our personal opinion on future developments.

[a] R, Wang, Prof. dr. F, Kapteijn, Prof. dr. J, Gascon
Catalysis Engineering, Chemical Engineering Department
Delft University of Technology
Van der Maasweg 9, 2629 HZ Delft, The Netherlands
E-mail: jorge.gascon@kaust.edu.sa.
[b] Prof. dr. J, Gascon
Advanced Catalytic Materials, KAUST Catalysis Center
King Abdullah University of Science and Technology
Thuwal 23955, Saudi Arabia.

Riming Wang received his MSc degree (2015) from College of Material Science and Engineering at Shandong University. In 2015, he joined the Department of Chemical Engineering at Delft University of Technology as a PhD student, under the supervision of Prof. Freek Kapteijn and Prof. Jorge Gascon. His research focuses on MOF-mediated catalyst engineering for CO_2 electrochemical reduction and MOF photocatalysis.

Freek Kapteijn (1952), MSc in Chemistry and Mathematics, received his PhD in 1980 at the University of Amsterdam. After post-doc positions (Coal Science) in Amsterdam and Nancy (ENSIC), he became Associate professor in Amsterdam. Moved to Delft University of Technology in 1992, was appointed 'Anthonie van Leeuwenhoek professor' in 1999, and chaired from 2008 till 2019 the Catalysis Engineering team. Holds the prestigious Golden Hoogewerff award and is among the highly cited 'Cross-Field' scientists 2018. Research interest focuses on the interplay of catalysis and engineering, comprising structured and multifunctional catalysts, adsorption, separation and (catalytic) membranes. Co-authored over 650 publications in peer-reviewed journals and as book chapters.

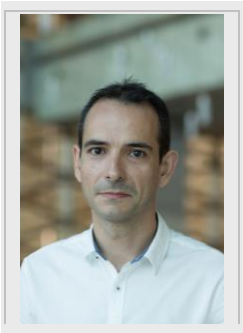

Born in Huesca (Spain) in 1977, Jorge received his MSc. in Chemistry in 2002 and his PhD in Chemical Engineering in 2006, both at the University of Zaragoza (Spain). He was post-doc (2006 to 2009), Assistant Professor (2010 to 2012), Associate Professor (2012 to 2014) and Antoni van Leeuwenhoek Professor (2014 – 2017) of Catalysis Engineering at TUDelft (NL). Since 2017 he is Professor of Chemical and Biological Engineering and Director at the KAUST Catalysis Center.

Gascon is a member of the board of the International Zeolite Association Commission on Metal Organic Frameworks. He has been the recipient of the 2013 ExxonMobil Chemical European Science and Engineering Award and he is a 2018 Clarivate Analytics highly cited researcher. His research focuses on the development of sustainable technologies for the production of chemicals, energy carriers and new environmental applications.

2. Main challenges for CO_2ER

CO_2 electrochemical reduction can be seen as a reversed process of fuel cells, and a lot of similarities are shared between these two processes, such as cell configuration, electrolyte, *etc*. CO_2ER with H-cell, one of the most popular cell configurations so far, features cathode and anode compartments filled with aqueous electrolyte and separated by a membrane. MOFs and MOF-derived catalysts are mostly particles, and are used as supported catalysts in CO_2ER cells. CO_2 approaches the catalytic sites through diffusion in aqueous phase, and several valuable products can be generated, such as CO, C_2H_4, HCOOH, oxalic acid, alcohols, *etc*. As proposed by Koper and coworkers,[10] the reduction of CO_2 starts with the formation of a $\cdot COO^-$ intermediate. Subsequent reaction with a proton-electron pair leads to the formation of $HCOO^-$, while the absorption of only a proton results in the formation of ·COOH, which will be further reduced to ·CO. On the one hand, if the ·CO intermediate is strongly bonded by the catalyst, for example Cu, it will be reduced to additional products. On the other hand, if the ·CO intermediate is weakly bonded (i.e. in case of Ag, Au or Zn) CO will desorb and become the main product.

The challenges of CO_2ER have been generally summarized and discussed,[1, 11] so we will only give a brief introduction to CO_2ER here, with specific emphasis on commercializing considerations.

2.1. Overpotential (voltage efficiency)

One of the key drawbacks that hinder the commercialization of CO_2ER is energy efficiency, which is primarily limited by the high overpotential of CO_2ER.

In electrochemistry, overpotential is the potential (voltage) difference between a half-reaction's reduction potential at thermodynamic equilibrium and the potential at which the redox reaction occurs. The existence of overpotential implies that more energy is required than thermodynamically needed to drive a given reaction, and this energy loss, usually in thermal form, directly affects voltage efficiency.

It is widely accepted that the overpotential for CO_2 electrochemical reduction originates from the sluggish kinetics to form a $\bullet CO_2^-$ intermediate.[11a, 11c] This step has a standard potential of -1.9 V *vs.* SHE and is the main reason for high overpotentials. This potential can be improved (lowered) by stabilizing the intermediate, which is one of the primary functions of catalysts.

2.2 Faradaic efficiency (FE)

Faraday efficiency is described as energy losses in the current term. Although all the current in CO_2ER is consumed to form products, the current directed toward undesirable reactions or products is usually considered as energy loss.

One primary undesirable product is H_2, generated by the competing hydrogen evolution reaction (HER) in the aqueous electrolyte. As a consequence, catalysts with high hydrogen overpotentials typically give favorable FE for CO_2ER.

From a commercialization perspective, the potential market of CO_2ER will be fuel and commodity chemicals, where oil derived products are now dominating. Taking the competition between CO_2ER derived chemicals and petrochemicals into consideration, it is clear that some CO_2ER products, for example CH_4, are economically unfavorable. Formation of these products should be avoided since the electricity cost to produce them will not be paid off.[1]

A scenario of CO_2ER commercialization would be the direct treatment of post-combustion gas from power plants, avoiding in this case expensive (and highly energy consuming) separation. These streams usually contain a relatively high concentration of unreacted O_2. Thus, CO_2ER catalyst for this specific application should be inactive toward oxygen reduction reaction (ORR).[12] Moreover, the ORR products are reactive O_2^- and H_2O_2 species sometimes, which offer a harmful environment for CO_2ER catalysts.[13]

2.3 CO_2 mass transport

One of the key limiting factors in aqueous-phase CO_2 conversion is the mass transfer of CO_2 to the cathode surface, especially given the low solubility of CO_2 in many electrolytes. In addition to catholyte CO_2 capacity, product bubble formation can disrupt the reaction system as well. Although the low solubility of CO_2 in aqueous phase can be overcome by using gas-diffusion electrodes (GDE), the current density of cathode GDEs may also be limited by the CO_2 flux to the catalyst. The CO_2 transport limit can be seen as the critical issue that hinders the enhancement of current density.[14] Configuration of electrochemical cells may largely influence the CO_2 transportation, and in turn influences the current density, thus it

should be noted that the comparison of current densities should take the cell configuration into consideration.[15]

2.4 Electrode stability

Stability is an essential criterion for commercial catalysts. Excellent stability can greatly reduce the operational costs.[16] In CO_2ER, the electrode stability requires not only the resistance to deactivation but also the resistance to impurities.[17] The long-time running of CO_2ER has been reported in several articles.[18] However, the resistance to impurities has not been widely covered. Again, taking the example of using the post-combustion gas from power plant as CO_2 feedstock, the post-combustion gas will contain a relatively high level of impurities, such as SO_x and NO_x, even after a primary treatment, and S has been identified as a harmful component to many electrocatalysts.[19] The electrolyte is another source of impurities.[11c, 20] In this regard, more research into impurity-resistant electrodes will be important. Additionally, electrode stability should be separated from system stability. For instance, electrode clogging because of the formation of bicarbonate crystals during CO_2ER is not related to the electrode itself but to the reactor system and such should be solved through system engineering.

3. MOF-related catalysts for CO_2ER

Table 1. Summary of CO_2ER performance with MOF-related materials.

Electro-catalyst[a]	Main product	Peak FE[b] (%)	Peak j_{total} (mA cm^{-2})	Peak potential [c] (V)	Electrolyte
CR-MOF[21]	Formic acid	~100	7.1	-0.78	0.5 M $KHCO_3$
Cu-BTC[22]	Oxalic acid	~51	19.22	-2.5 vs Ag/Ag^+	0.01 M TBATFB in DMF
ZIF-8[23]	CO	65	~3	-1.14	0.5 M NaCl
ZIF-8[24]	CO	81	8.5	-1.1	0.25 M K_2SO_4
ZIF-108[24]	CO	52	24.6	-1.3	0.25 M K_2SO_4
Cu-BTC[25]	ethanol	10.3	10	-0.28	0.5 M $KHCO_3$
Ligand-doped –ZIF-8[26]	CO	90	10.1	-1.2	0.1 M $KHCO_3$
Re-MOF[27]	CO	93	>2	-1.6 vs NHE	0.1 M TBAH in CH_3CN+5% trifluoroethanol
ZIF-BTC[28]	CH_4	80	3.1	-2.2 vs Ag/Ag^+	$BmimBF_4$
Fe_MOF-525[29]	CO	50	~6	-1.3 vs NHE	1 M $TBATF_6$ in DMF
PCN-222(Fe)[30]	CO	91	1.2	-0.6	0.5 M $KHCO_3$
Cu_2(CuTCPP) nanosheet[31]	$HCOO^-$	68.4	~4.5	-1.55 vs Ag/Ag^+	CH_3CN with 1 M H_2O and 0.5 M $EMIMBF_4$
$Al_2(OH)_2$TCPP-Co MOF[32]	CO	76	~1	-0.7	0.5 M $KHCO_3$
Ag_2O/layered ZIF[33]	CO	~80	32	-1.3	0.25 M K_2SO_4
Cu-SIM NU-1000[34]	$HCOO^-$	28	1.2	-0.82	0.1 M $NaClO_4$
Cu_2O@Cu-MOF[35]	CH_4	63.2	-14	-1.71	0.1 M KHCO3
OD-Cu/C[36]	CH_3OH	~43.2	~8.9	-0.3	0.1 M $KHCO_3$
MOF-derived Cu NPs[37]	CH_4	~50	7.5	-1.3	0.1 M $KHCO_3$
ZIF-8 derived Fe-N active sites[38]	CO	93	5.2	-0.43	1 M $KHCO_3$
Ni SA/N-C[39]	CO	71.9	10.48	-1.0	0.5 M $KHCO_3$
N-coordinated Fe[40]	CO	93	2.8	-0.58	0.1 M $KHCO_3$
Low-CN Cu clusters[41]	C_2H_4	45	262	-1.07	1 M KOH
N-coordinated Co[42]	CO	94	18.1	-0.63	0.5 M $KHCO_3$
MOF-derived In-Cu bimetallic oxides[43]	CO	92.1	11.2	-0.8	0.5 M $KHCO_3$
ZIF-8 derived NC[44]	CO	78	1.1	-0.93	0.1 M $KHCO_3$
ZIF-8 derived NC[45]	CO	95.4	1	-0.5	0.5 M $KHCO_3$
Pyrolyzed ZIF/MWCNT[46]	CO	100	7.7	-0.86	0.1 M $NaHCO_3$

[a] The MOF-related catalysts mentioned in this table were used in a supporting manner. A list of abbreviations is presented at the end.

[b] Peak FE represents the FE of main products.

[c] Peak potential represents the potential where peak FE occurs, and is against RHE unless specifically noted.

3.1. MOF as electrocatalysts

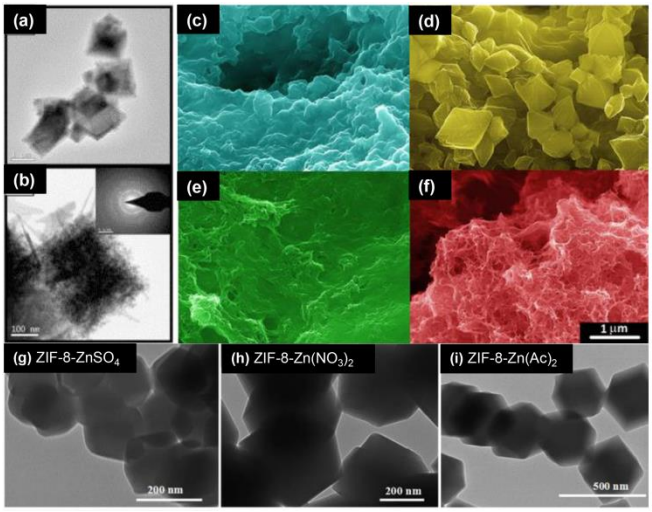

Figure 1. Representative electron micrograph of directly using MOF as electrocatalyst. TEM image of (a) lower and (b) higher magnification, SAED pattern (inset) of Cu-BTC;[22] SEM images at 25 000× magnification of (a) HKUST-1, (b) CuAdeAce, (c) CuDTA, and (d) CuZnDTA, not real colors;[25] TEM images for ZIF-8-$ZnSO_4$ (g), ZIF-8-$Zn(NO_3)_2$ (h), and ZIF-8-$Zn(Ac)_2$ (i).[23]

MOFs, combining the favorable characteristics of heterogeneous and homogeneous catalysts, have been explored as a novel class of model catalytic materials for understanding the electrochemical CO_2 reduction.

The application of MOF-related catalysts for CO_2 electrochemical reduction started in 2012,[21] when a copper rubeanate metal-organic framework (CR-MOF) was prepared by Hinogami *et al.* to electrochemically reduce CO_2 into valuable products. With an onset potential of ~200 mV more positive than that of a Cu electrode in the aqueous electrolyte, formic acid (HCOOH) was virtually the only CO_2 reduction product (FE = ~100%), whereas various products were generated on a Cu electrode. The partial current of HCOOH by CR-MOF electrode was ~7.1 mA cm^{-2}, which was also higher than for the Cu electrode.

Kumar *et al.*, also in 2012, reported cyclic voltammetry (CV) studies in 0.1 M KCl of Cu-BTC films on glassy carbon electrodes.[22] Well-defined Cu(II)/Cu(I) and Cu(I)/Cu(0) reversible redox responses were observed. The MOF film was then studied as electrocatalyst in N,N-dimethylformamide (DMF). The production of oxalic acid was confirmed by GC-MS with a FE of ~51% and a total current density of 19 mA cm^{-2}.

Following these pioneering works, additional MOF-based catalysts have been investigated for CO_2ER. ZIF-8, an archetypical MOF material, was synthesized with various zinc sources by Wang *et al.* and used as electrocatalyst for CO_2 reduction to CO.[23] ZIF-8 prepared with $ZnSO_4$ delivered the best catalytic activity towards CO_2 electroreduction, with a FE toward CO (FE_{CO}) of 65% and a total current density (j_{Total}) of ~3 mA cm^{-2}, establishing a relation between the CO_2ER performance and synthetic zinc sources. The main catalytic active sites were claimed to be the discrete Zn nodes in ZIF-8.

Jiang *et al.* further identified the imidazolate ligands coordinated with the Zn(II) center in ZIFs as the catalytic sites of ZIFs for CO_2ER with the help of in-situ X-ray absorption spectroscopy (XAS) measurements and density functional theory (DFT) calculations.[24] They investigated ZIFs with the same sodalite topology and different organic ligands, including ZIF-8, ZIF-108, ZIF-7, and SIM-1 for CO_2ER in aqueous electrolyte. ZIF-8 showed the highest FE_{CO} of 81.0% at -1.1 V *vs.* RHE among all the ZIF catalysts, and the CO current density could reach as high as 12.8 mA cm^{-2} at -1.3 V *vs*. RHE over ZIF-108.

The effect of the linker on CO_2ER was also investigated[25] by Albo *et al.* Four Cu-based MOFs, namely, 1) Cu-BTC (HKUST-1); 2) Cu-AdeAce; 3) Cu-DTA mesoporous metal-organic aerogel (MOA); and 4) CuZn-DTA MOA, were synthesized and supported on gas diffusion electrodes. The MOF-based electrodes showed electrocatalytic efficiency for the production of methanol and ethanol in the liquid phase. The maximum cumulative FE for CO_2 conversion was measured at Cu-BTC based electrodes, which was 15.9 % at a current density of 10 mA cm^{-2}. It was demonstrated that MOFs with coordinately unsaturated metal sites were favorable for the enhancement of the electrocatalytic reduction of CO_2 to alcohols. Furthermore, Cu-BTC based electrodes showed stable electrocatalytic performance for 17 h.

In addition to the structural effect, the linker of MOFs can also be functionalized to boost the catalytic activity. The poor conductivity of MOFs largely hinders their direct application as electrocatalysts, thus, Dou *et al.* reported a general strategy of ligand doping to enhance charge transfer, thereby improving the electrocatalytic activity.[26] A strong electron-donating molecule, 1,10-phenanthroline, was introduced into ZIF-8 as CO_2 reduction electrocatalyst. Experimental and theoretical results suggested that the electron-donating nature of phenanthroline enabled charge transfer, which facilitated the generation of •COOH. As a consequence, the ligand-doped ZIF-8 showed an FE_{CO} of 90% and a j_{Total} of 10.1 mA cm^{-2}, both significantly improved compared with pristine ZIF-8.

Ye *et al.* deposited a highly oriented monolithic Re-based MOF thin film onto a conductive FTO electrode using liquid-phase epitaxy.[27] The MOF film was grown exclusively along the [001] direction, and exhibited a high FE_{CO} of ~93% when operated as an electrocatalyst for the reduction of CO_2, with a current density exceeding 2 mA cm^{-2}.

As discussed above, the overpotential is one of the key issues which needs to be addressed in CO_2ER. A combination of ionic liquids (ILs) as the electrolyte and Zn-BTC as the catalyst was applied by Kang *et al.* as a strategy to lower overpotentials in CO_2ER,[28] which was the first work combining a MOF electrode and pure IL electrolyte in this field. The Zn-BTC electrode showed a higher selectivity to CH_4 (>80%) and higher current density (3 mA cm^{-2}) at mild overpotentials (250 mV), than the commonly used metal electrodes.

3.2 MOFs as active phase supports

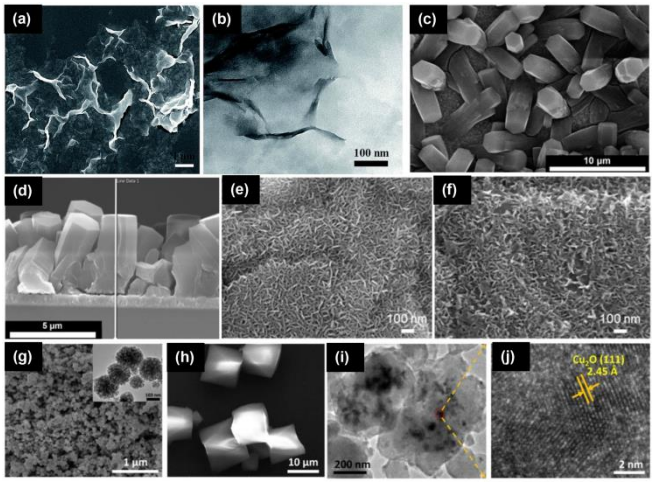

Figure 2. Representative electron micrograph of using MOF as catalyst supports. (a) SEM image and (b) TEM image of Cu_2(CuTCPP) nanosheets;[31] Top-view SEM images (c) and cross-sectional SEM image (d) of the Cu-SIM NU-1000 thin film;[34] SEM images of the MOF catalyst film before (e) and after electrolysis (f) revealing the retention of the plate-like morphology;[32] (g) SEM and TEM (inset in g) images of Cu_2O spheres, (h) SEM image of Cu-MOF, (i) TEM and (j) HRTEM images of Cu_2O@Cu-MOF after reacting for 12 h.[35]

In addition to the direct application as electrocatalysts, the unique textural properties of MOFs also offer a number of opportunities for their application as active phase supports for CO_2ER.

Porphyrin-based molecular catalysts have been widely used in CO_2ER.[47] The significance of molecular catalyst immobilization was highlighted by Hu *et al.* by comparing the performance of cobalt meso-tetraphenylporphyrin (CoTPP) in CO_2ER under both supported and unsupported conditions.[48] CoTPP performed poorly as a homogeneous electrocatalyst giving low product selectivity at a high overpotential, while a remarkable catalytic activity enhancement was seen with CO_2 selectively forming CO (> 90%) at a low overpotential upon directly immobilizing CoTPP onto carbon nanotubes. Kramer *et al.* demonstrated that the immobilization agent had an effect on the molecular catalyst's performance by comparing the CO_2ER activity of cobalt phthalocyanine (CoPc) supported on edge-plane graphite and poly-4-vinylpridine (P4VP) thin films.[49] CoPc embedded in P4VP matrix displayed improved FE_{CO} and turnover frequency, which was attributed to the chemical coordination environment provided by the P4VP polymer matrix.

Hod *et al.* used Fe-porphyrin as CO_2 reduction catalyst, which was incorporated into MOF-525 as both a structural and functional element.[29] MOF-525 was first deposited onto a conductive ITO substrate, and then Fe-porphyrin was formed via a post-metalation strategy. The approach yielded a high surface coverage of electrochemically addressable Fe-porphyrin sites (~1015 sites cm^{-2}), forming a mixture of CO and H_2 in roughly equal amounts (FE_{CO} = ~50 %) as products with a j_{Total} of ~6 mA cm^{-2}. In spite of the low FE of CO_2ER, these results demonstrated that porphyrins can be electrochemically accessed when incorporated into a MOF structure.

Electroactive porphyrins can also be used as ligands to form MOFs. Dong *et al.* rationally introduced a Fe-TCPP porphyrin to form PCN-222(Fe) as CO_2ER catalyst.[30] After dip-coating onto carbon substrate, the composite catalyst PCN-222(Fe)/C (mass ratio = 1:2) exhibited a maximum 91% FE_{CO} with 494 mV overpotential (where j_{Ttoal} = 1.2 mA cm^{-2}) in an aqueous solution, achieving a TOF of 0.336 $site^{-1}$ s^{-1}. The catalyst was found to retain its crystallinity and stability after 10 h of electrolysis at −0.60 V versus RHE (average FE_{CO} = 80.4%).

Wu *et al.* used porphyrinic MOF nanosheets for CO_2ER.[31] The Cu_2(CuTCPP) nanosheets were cathodized on FTO glasses, and exhibited significant activity for formate production with a FE of 68.4% at -1.55 V *vs.* Ag/Ag^+. Moreover, the C–C coupling product acetate was also generated from the same catalyst at a voltage range of 1.40 - 1.65 V with the total liquid product FE of 38.8 - 85.2%. Characterization results showed the instability of Cu_2(CuTCPP), with Cu(II) being transformed into CuO, Cu_2O and Cu_4O_3, which significantly catalyzed CO_2 to formate and acetate.

Kornienko *et al.* employed an aluminium porphyrin-based MOF-55,[32] comprising cobalt porphyrin active sites, for the electrocatalytic reduction of CO_2 to CO. An aluminium oxide thin film was first deposited via atomic layer deposition (ALD) as metal precursor, followed by subsequent MOF formation through the reaction of the coated aluminium oxide with the linker under solvothermal conditions. The thickness of the precursor could easily be controlled by the number of ALD cycles, thereby controlling the thickness of catalyst layers. The performance of the resulting MOF catalyst initially improved with increasing film thickness until reaching a maximum of ~2.8 mA cm^{-2}, and the appearance of maximum performance possibly indicated a trade-off between electron and mass transport. The optimized catalyst thickness exhibited a FE_{CO} production of up to 76 % in a 7 h test.

In addition to molecular catalysts, MOFs have also been used for supporting metal nanoparticles in CO_2ER. Jiang *et al.* reported the construction of Ag_2O/layered ZIF composite structure by mixing pre-synthesized layered ZIF-7 with $AgNO_3$ aqueous solution, followed by refluxing at 100 °C.[33] Ag_2O/layered ZIF composite showed much higher FE_{CO} (~80 %) and j_{CO} (~32 mA cm^{-2}) than the layered ZIF or Ag/C alone. The performance enhancement was attributed to the synergistic effect between Ag_2O nanoparticles and the layered ZIF, as well as the facilitated mass transport by the high specific surface area of Ag_2O/layered ZIF.

Kung *et al.* embedded copper nanoparticles into a thin film of NU-1000,[34] by first installing single-site Cu(II) into the NU-1000 thin film followed by electrochemical reduction of Cu(II) to metallic Cu. The obtained Cu nanoparticles were electrochemically addressable and exhibited a moderate electrocatalytic activity with a maximum FE toward $HCOO^-$ of 28 % and -1.2 mA cm^{-2} at -0.82 V *vs.* RHE. Both the crystallinity and morphology of the thin film remained unchanged after electrocatalysis. The authors also found that the particle sizes were largely dependent on the pore size of the MOF, which might offer an opportunity to achieve tunable catalyst sizes through this pore confinement effect of MOFs.

In a recent study, Tan *et al.* reported a tailor-made Cu_2O@Cu-MOF electrocatalyst,[35] by in-situ etching Cu_2O spheres with H3BTC to form a Cu-MOF shell. The as-prepared electrocatalyst resulted in an intriguing performance towards the formation of hydrocarbons from CO_2, with a high FE toward CH_4 and C_2H_4 of 79.4%, particularly, the FE of CH_4 as high as 63.2% at −1.71 V.

3.3 MOF as electrocatalyst precursors

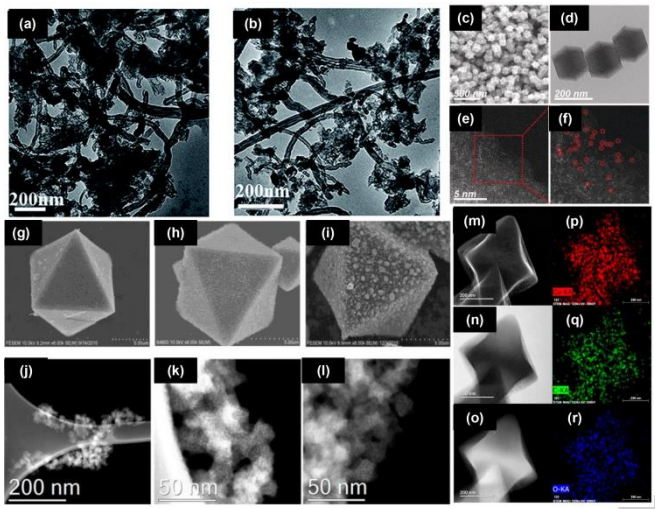

Figure 3. Representative electron micrograph of using MOF as catalyst precursors. TEM images of (a) ZIF–CNT–FA-p, and (b) ZIF–Fe–CNT–FA-p;[46] (c) SEM and (d) TEM images of N-coordinated Co. (e-f) Magnified HAADF-STEM images of N-coordinated Co showing the atomic dispersion of Co atoms;[42] (g-i) SEM images of the OD-Cu/C processed with different temperature;[36] The HAADF-STEM images of (j-l) Fe–N–C;[40] Structural investigations of as-fabricated HKUST-1 by (m) SEM, (n) TEM bright field image, (o) TEM HAADF, and (p-r) TEM EDS.[41]

Although quite a few works using MOFs directly as catalysts claimed that the MOF catalysts showed good stability during test, a lot of them failed to conduct post-reaction analysis to confirm these statements.[50] Indeed, stability is a serious issue for MOFs, especially under the highly negative potentials usually applied in CO_2ER. These potentials are more negative than the reduction potential of many metals used in MOF synthesis (see Table 2). In this spirit, using a MOF as catalyst precursor can be a favorable way to produce a stable and efficient catalyst.

Table 2. Standard electrode potentials of common metal nodes in MOFs.[51]

Half reaction	Potential (V vs. RHE)
$Co^{3+} + e^- \rightleftharpoons Co^{2+}$	1.82
$Ag^+ + e^- \rightleftharpoons Ag$	0.8
$Fe^{3+} + e^- \rightleftharpoons Fe^{2+}$	0.77
$Cu^+ + e^- \rightleftharpoons Cu$	0.52
$O_2 + 2H_2O + 4e^- \rightleftharpoons 4OH^-$	0.4
$Cu^{2+} + 2e^- \rightleftharpoons Cu$	0.34
$Cu^{2+} + e^- \rightleftharpoons Cu^+$	0.15
$2H^+ + 2e^- \rightleftharpoons H_2$	0
$Fe^{3+} + 3e^- \rightleftharpoons Fe$	-0.04
$Ni^{2+} + 2e^- \rightleftharpoons Ni$	-0.25
$Co^{2+} + 2e^- \rightleftharpoons Co$	-0.29
$Fe^{2+} + 2e^- \rightleftharpoons Fe$	-0.41
$Cr^{3+} + e^- \rightleftharpoons Cr^{2+}$	-0.42
$Cr^{3+} + 3e^- \rightleftharpoons Cr$	-0.74
$Zn^{2+} + 2e^- \rightleftharpoons Zn$	-0.76
$Ti^{3+} + 3e^- \rightleftharpoons Ti$	-1.37
$Zr^{4+} + 4e^- \rightleftharpoons Zr$	−1.45
$Ti^{2+} + 2e^- \rightleftharpoons Ti$	-1.63
$Al^{3+} + 3e^- \rightleftharpoons Al$	-1.66

The decomposition of MOFs under controlled conditions usually leads to the clustering of its metal component into small nanoparticles. Zhao *et al.* synthesized oxide-derived Cu/carbon (OD Cu/C) catalysts by facile carbonization of Cu-BTC MOF (HKUST-1).[36] The resulting materials exhibited highly selective CO_2 reduction to alcohols with total FE of 71.2% at -0.7 V *vs.* RHE. High yields to methanol and ethanol were achieved on OD Cu/C-1000 with the peak production rates of 12.4 mg L^{-1} h^{-1} at -0.3V and 13.4 mg L^{-1} h^{-1} at -0.7V, respectively. Notably, the onset potential for C_2H_5OH formation was among the lowest overpotentials reported to date for the CO_2 reduction to C_2H_5OH. The improvement in activity and selectivity of the oxide-derived Cu/carbon were attributed to the synergistic effect between the highly dispersed copper and the matrix of porous carbon.

Kim *et al.* used an electrochemical reduction strategy to decompose MOFs,[37] obtaining an efficient electrocatalyst for the synthesis of CH_4. Cu-based MOF-74 was chosen as the precursor, which was electrochemically reduced to Cu nanoparticles (NPs). The porous structure of the MOF serves as a template for the synthesis of isolated Cu NPs with high current densities and high FE toward CH_4 in the electrochemical CO_2 reduction reaction. The MOF-derived Cu NPs resulted in a

FE_{CH4} >50% and a 2.3-fold higher current density at -1.3 V *vs.* RHE than commercially available Cu NPs.

Besides metal nanoparticles, MOF-mediated synthesis can also act as a method to generate isolated metal-nitrogen sites with high exposure of active sites for efficient catalysis. Ye *et al.* fabricated isolated iron-nitrogen sites, located on the surface of carbon matrix, through the pyrolysis of ammonium ferric citrate (AFC)/ZIF-8 composites.[38] The AFC/ZIF-8 composite was synthesized by reacting the Zn precursor solution, in which the AFC was also dissolved, with 2-methylimidazole solution, followed by cleaning, centrifuging, and drying. The highly exposed iron-nitrogen sites demonstrated high selectivity to CO (peak FE_{CO} = 93 %) and high activity (j_{CO} = 9.5 mA cm^{-2}).

Zhao *et al.* adopted Ni ion exchanged ZIF-8 to assist the preparation of a catalyst containing single Ni sites for efficient CO_2 electroreduction.[39] The synthesis was based on an inexpensive ionic exchange between Zn nodes and adsorbed Ni ions within the cavities of the MOF, which was followed by pyrolysis of the ion-exchanged MOF. This single-atom catalyst exhibited an outstanding turnover frequency for CO_2 electroreduction (5273 h^{-1}), with a FE_{CO} of over 71.9% and a j_{Total} of 10.48 mA cm^{-2} at an overpotential of 890 mV.

Pan *et al.* studied the reactivity and structure of atomically dispersed M-N_4 (M = Fe and Co) single sites in CO_2ER. Nitrogen coordinated Fe or Co single site atomically dispersed into a carbon matrix (M-N-C) were prepared by using MOF precursors which were further studied as model catalysts.[40] Fe was intrinsically more active than Co in M-N_4 for the reduction of CO_2 to CO, in terms of a higher FE_{CO} (93% *vs.* 45%) and current density. First principle computations elucidated that the M-N_{2+2}-C_8 moieties, which were distributed at the edge of carbon matrix and bridged two adjacent armchair-like graphitic layers, were the active sites for the CO_2ER.

Selectivity is one of the key issues faced by CO_2ER, especially when Cu-based catalysts are used. Nam *et al.* reported a strategy involving MOF-regulated Cu cluster formation that shifted CO_2 electroreduction with Cu based catalysts towards multiple-carbon products.[41] The symmetric paddle-wheel Cu dimer secondary building block of HKUST-1 was distorted to an asymmetric motif by separating adjacent benzene tricarboxylate moieties using thermal treatment. By varying materials processing conditions, the asymmetric local atomic structure, oxidation state and bonding strain of Cu dimers were modulated. The formation of Cu clusters with low coordination numbers from distorted Cu dimers in HKUST-1 was observed during CO_2 electroreduction, leading to a *FE* toward C_2H_4 of 45%. The enhanced performance was closely related to maintaining a low Cu-Cu coordination number among the Cu clusters during the reaction.

Another example of regulating coordination number to tune the selectivity was reported by Wang *et al.*[42] A series of atomically dispersed Co catalysts with different nitrogen coordination numbers were prepared for the CO_2ER. The best catalyst, atomically dispersed Co with two-coordinate nitrogen atoms, achieved both high selectivity (FE_{CO} = 94 %) and superior activity (j_{Total} = 18.1 $mAcm^{-2}$) at an overpotential of 520 mV. The CO formation turnover frequency reached a record value of 18200 h^{-1}. These results demonstrated that lower a coordination number facilitated activation of CO_2 to the •COO^- intermediate and hence enhanced CO_2ER activity.

Very recently, Guo *et al.* introduced a new method to tune the CO_2ER selectivity via MOF-derived bimetallic oxide catalyst.[43] MOF-derived In-Cu bimetallic oxides were synthesized by pyrolysis of a Cu-In bimetallic MOF. By controlling In-Cu ratios, the FE_{CO} could reach 92.1%, along with a j_{Total} of 11.2 mA cm^{-2}. The excellent performance was mainly attributed to stronger CO_2 adsorption, higher electrochemical surface area and lower charge transfer resistance by the bimetallic catalyst.

Besides metal-based catalysts, a carbon-rich organic linker, combined with the low-boiling point of some metal nodes, such as Zn, make MOFs a promising precursor to produce carbon-based electrocatalysts.[52] Following this strategy, Wang *et al.* synthesized a nitrogen-doped carbon (NC), through the pyrolysis of the well-known metal-organic framework ZIF-8.[44] The resulting NC-based CO_2ER electrode showed a FE_{CO} as high as ~78%. It was also found that the pyrolysis temperature determined the amount and the accessibility of N species in the carbon electrode, in which pyridinic-N and quaternary-N species played key roles in the selective formation of CO. Generally the materials derived from Zn-based ZIFs are nothing less than nitrogen containing carbons and are active without other metal addition. Therefore it should be kept in mind to benchmark their performance against those materials prepared via other routes.[53]

The pyrolysis temperature effect and the mechanism in the ZIF-8-derived NC was further studied by Zheng *et al.*[45] NC catalysts were prepared by decomposing ZIF-8 at different temperatures in argon. The catalytic performances showed that the higher pyrolysis temperature resulted in a better CO_2ER activity. The NC catalyst with the best performance achieved high selectivity with 95.4 % FE_{CO} at −0.5 V *vs*. RHE. The catalyst also maintained stability during 20 h operation, after which the FE_{CO} was still greater than 90%. The experiments showed that a higher pyrolysis temperature reduced the total nitrogen contents but changed the nature and density of N-species. DFT calculations revealed that higher pyrolysis temperature led to enhanced activity by promoting the formation of pyridinic N, which provided more efficient active sites.

To relieve the electron transportation limit with MOF-mediated approach, Guo *et al.* synthesized a composite material by co-pyrolysis of in-situ grown ZIF-8 on multi-walled carbon nanotubes (MWCNTs) substrate.[46] This composite could selectively catalyze the electrochemical reduction of CO_2 to CO in aqueous solution with ~100 % FE and a current density up to 7.7 mA cm^{-2} at an overpotential of 740 mV. By comparison, the pyrolyzed ZIF-8 without MWCNT only showed a FE_{CO} of ~50%. Addition of Fe to the ZIF could lower the overpotential, but also changed the selectivity. The MWCNT support was crucial to achieving superior efficiency, by enhancing electron transport through the MWCNT network and simultaneously expediting the CO_2 transport in the mesoporous structure constructed by the MWCNTs.

4. Concluding remarks

CO_2ER is widely regarded as one of the most promising technologies to solve the CO_2 emission issue, though it is still faced by several challenges on the path toward commercialization. In this work, we have summarized recent works on CO_2 electroreduction with MOFs and MOF mediated catalysts. Generally speaking, the main advantages of MOFs in CO_2ER originate from their unique textural and structural properties. When MOFs are used directly as catalysts for CO_2ER, the atomically dispersed metal nodes can offer highly active sites, and the organic linkers can also be modified into catalytic sites or charge transfer agents. The porous structure, put up by the metal nodes and organic linkers, makes catalytic sites more accessible to CO_2 either if catalysis takes place on the MOF itself or on supported species. Moreover, the compatibility of MOFs with ILs facilitates their application in this medium. The use of MOFs as catalyst precursors usually leads to highly dispersed metal particles or carbon-based catalysts, maximizing catalyst utilization. The homogeneously dispersed metal sites can be inherited by the MOF-derived catalysts to form efficient single-site catalysts with unprecedented TOFs. And the highly tunable building blocks of MOFs enable the formation of bi-metallic structures, providing a facile route to the synthesis of metal alloys, opening the door to breaking scaling relationships in CO_2ER.[10]

Although remarkable results have been reported with MOF-related catalysts, there are still issues that need to be carefully addressed in future research. Stability is one of the most concerning issues for CO_2ER. While most authors have claimed that pristine MOFs based on easily reducible metals are stable under reaction conditions, the catalyst stability has only been confirmed in a few cases by post-analysis characterization.[30, 32, 34-35] Here, we would like to clarify that stability of the crystalline MOF does not necessarily need to be an issue. Indeed, from an application point of view, electrochemical reduction of MOFs to form small metal nanoparticles may render very interesting catalytic systems. However, as scientists, we should make sure that we do not jump into wrong conclusions by attributing the observed catalytic performance to the MOF scaffold.

As it is the case in thermal catalysis, probably the most exciting results in terms of performance have been reported for MOF-derived catalysts.[7a, 54] We believe that this route offers great possibilities for the further engineering of CO_2ER catalysts and for the optimization of metal use in catalysis, an aspect that may become critical if CO_2 electrolyzers are massively applied.

Last but not least, it is fair to admit that so far most catalytic results have been reported using aqueous electrolytes and semi-batch experiments, where only low current densities can be achieved due to the low solubility of CO_2 in aqueous phase. We are sure that, as it is already happening for “traditional” electrocatalysts, MOF-derived systems will soon be tested under commercially more relevant conditions by making use of gas-diffusion electrochemical cells in which high current densities (>100 mA cm^{-2}) have been achieved.[55] Through carbon capture technologies from point sources liquid CO_2 will become available at pressures exceeding 100 bar and solubility may not be limiting any more. Also aspects of molecular and electron transport require careful attention, as shown by Guo *et al.*[46] Overall, we are confident that MOF-related catalysts engineering when combined with system integration of CO_2ER, will mark a substantial contribution to the field of electrocatalytic CO_2 reduction.

Abbreviations

BTC	Benzene-1,3,5-Tricarboxylate
CN	Coordination Number
CR-MOF	Copper Rubeanate Metal-Organic Framework
FE	Faradaic efficiency
HER	Hydrogen evolution reaction
MWCNT	Multi-walled Carbon Nanotube
NC	Nitrogen-doped Carbon
ORR	Oxygen reduction reaction
Pc	Phthalocynine
P4VP	Poly-4-vinylpridine
PCN	Porous Coordination Network
RHE	Reversible hydrogen electrode
SHE	Standard hydrogen electrode
SIM	Substituted Imidazolate Material
TBAH	Tetrabutylammonium hydroxide
TCPP	Tetrakis(4-carboxyphenyl)porphyrin
TOF	Turnover frequency
ZIF	Zeolitic Imidazolate Framework

Acknowledgements

The authors would like to acknowledge China Scholarship Council for financial support.

Keywords: Metal-organic frameworks • Electrochemical CO_2 reduction • MOF-mediated synthesis • MOF-related catalyst

[1] C. Chen, J. F. K. Kotyk, S. W. Sheehan, Chem 2018, 4, 2571-2586.

[2] A. Dokania, A. Ramirez, A. Bavykina, J. Gascon, ACS Energy Letters 2019, 4, 167-176.

[3] Hori, Y. (2010). CO2 ‐ reduction, catalyzed by metal electrodes. In Handbook of Fuel Cells (eds W. Vielstich, A. Lamm, H. A. Gasteiger and H. Yokokawa).

[4] a) D. Gao, F. Cai, G. Wang, X. Bao, Current Opinion in Green and Sustainable Chemistry 2017, 3, 39-44; b) M. Ma, W. A. Smith, in Anisotropic and Shape-Selective Nanomaterials: Structure-Property Relationships (Eds.: S. E. Hunyadi Murph, G. K. Larsen, K. J. Coopersmith), Springer International Publishing, Cham, 2017, pp. 337-373; c) L. Zhang, Z.-J. Zhao, J. Gong, Angewandte Chemie International Edition 2017, 56, 11326-11353.

[5] a) A. Corma, H. García, F. X. Llabrés i Xamena, Chemical Reviews 2010, 110, 4606-4655; b) A. U. Czaja, N. Trukhan, U. Müller, Chemical Society Reviews 2009, 38, 1284-1293; c) A. Dhakshinamoorthy, H. Garcia, Chemical Society Reviews 2012, 41, 5262-5284; d) D. Farrusseng, S. Aguado, C. Pinel, Angewandte Chemie International Edition 2009, 48, 7502-7513; e) D. Feng, Z.-Y. Gu, J.-R. Li, H.-L. Jiang, Z. Wei, H.-C. Zhou, Angewandte Chemie International Edition 2012, 51, 10307-10310; f) H. Furukawa, K. E. Cordova, M. O’Keeffe, O. M. Yaghi,

Science 2013, 341, 1230444; g) S. L. James, Chemical Society Reviews 2003, 32, 276-288; h) J. Lee, O. K. Farha, J. Roberts, K. A. Scheidt, S. T. Nguyen, J. T. Hupp, Chemical Society Reviews 2009, 38, 1450-1459; i) J. Liu, L. Chen, H. Cui, J. Zhang, L. Zhang, C.-Y. Su, Chemical Society Reviews 2014, 43, 6011-6061; j) Y. Liu, W. Xuan, Y. Cui, Advanced Materials 2010, 22, 4112-4135; k) L. Ma, C. Abney, W. Lin, Chemical Society Reviews 2009, 38, 1248-1256; l) L. Ma, J. M. Falkowski, C. Abney, W. Lin, Nature Chemistry 2010, 2, 838; m) K. Schlichte, T. Kratzke, S. Kaskel, Microporous and Mesoporous Materials 2004, 73, 81-88; n) J. S. Seo, D. Whang, H. Lee, S. I. Jun, J. Oh, Y. J. Jeon, K. Kim, Nature 2000, 404, 982-986; o) C.-D. Wu, A. Hu, L. Zhang, W. Lin, Journal of the American Chemical Society 2005, 127, 8940-8941; p) H.-C. Zhou, J. R. Long, O. M. Yaghi, Chemical Reviews 2012, 112, 673-674; q) L. Alaerts, E. Séguin, H. Poelman, F. Thibault-Starzyk, P. A. Jacobs, D. E. De Vos, Chemistry – A European Journal 2006, 12, 7353-7363; r) M. H. Alkordi, Y. Liu, R. W. Larsen, J. F. Eubank, M. Eddaoudi, Journal of the American Chemical Society 2008, 130, 12639-12641; s) S.-H. Cho, B. Ma, S. T. Nguyen, J. T. Hupp, T. E. Albrecht-Schmitt, Chemical Communications 2006, 2563-2565; t) D. Dang, P. Wu, C. He, Z. Xie, C. Duan, Journal of the American Chemical Society 2010, 132, 14321-14323; u) A. Dhakshinamoorthy, M. Alvaro, H. Garcia, Catalysis Science & Technology 2011, 1, 856-867; v) A. Dhakshinamoorthy, M. Alvaro, H. Garcia, Chemical Communications 2012, 48, 11275-11288; w) A. Dhakshinamoorthy, H. Garcia, Chemical Society Reviews 2014, 43, 5750-5765; x) J. Gascon, U. Aktay, M. D. Hernandez-Alonso, G. P. M. van Klink, F. Kapteijn, Journal of Catalysis 2009, 261, 75-87; y) S. Horike, M. Dincă, K. Tamaki, J. R. Long, Journal of the American Chemical Society 2008, 130, 5854-5855; z) A. J. Howarth, Y. Liu, P. Li, Z. Li, T. C. Wang, J. T. Hupp, O. K. Farha, Nature Reviews Materials 2016, 1, 15018; aa) Y.-B. Huang, J. Liang, X.-S. Wang, R. Cao, Chemical Society Reviews 2017, 46, 126-157; ab) H.-L. Jiang, T. Akita, T. Ishida, M. Haruta, Q. Xu, Journal of the American Chemical Society 2011, 133, 1304-1306; ac) U. Mueller, M. Schubert, F. Teich, H. Puetter, K. Schierle-Arndt, J. Pastré, Journal of Materials Chemistry 2006, 16, 626-636; ad) M. Ranocchiari, J. A. v. Bokhoven, Physical Chemistry Chemical Physics 2011, 13, 6388-6396; ae) F. Song, C. Wang, J. M. Falkowski, L. Ma, W. Lin, Journal of the American Chemical Society 2010, 132, 15390-15398; af) C.-Y. Sun, S.-X. Liu, D.-D. Liang, K.-Z. Shao, Y.-H. Ren, Z.-M. Su, Journal of the American Chemical Society 2009, 131, 1883-1888; ag) P. Valvekens, F. Vermoortele, D. De Vos, Catalysis Science & Technology 2013, 3, 1435-1445; ah) F. Vermoortele, B. Bueken, G. Le Bars, B. Van de Voorde, M. Vandichel, K. Houthoofd, A. Vimont, M. Daturi, M. Waroquier, V. Van Speybroeck, C. Kirschhock, D. E. De Vos, Journal of the American Chemical Society 2013, 135, 11465-11468; ai) C.-D. Wu, W. Lin, Angewandte Chemie International Edition 2007, 46, 1075-1078; aj) Q. Yang, Q. Xu, H.-L. Jiang, Chemical Society Reviews 2017, 46, 4774-4808; ak) M. Zhao, K. Deng, L. He, Y. Liu, G. Li, H. Zhao, Z. Tang, Journal of the American Chemical Society 2014, 136, 1738-1741; al) L. Zhu, X.-Q. Liu, H.-L. Jiang, L.-B. Sun, Chemical Reviews 2017, 117, 8129-8176; am) Q.-L. Zhu, J. Li, Q. Xu, Journal of the American Chemical Society 2013, 135, 10210-10213; an) R.-Q. Zou, H. Sakurai, Q. Xu, Angewandte Chemie International Edition 2006, 45, 2542-2546.

[6] a) J. Gascon, A. Corma, F. Kapteijn, F. X. Llabrés i Xamena, ACS Catalysis 2014, 4, 361-378; b) S. M. J. Rogge, A. Bavykina, J. Hajek, H. Garcia, A. I. Olivos-Suarez, A. Sepúlveda-Escribano, A. Vimont, G. Clet, P. Bazin, F. Kapteijn, M. Daturi, E. V. Ramos-Fernandez, F. X. Llabrés i Xamena, V. Van Speybroeck, J. Gascon, Chemical Society Reviews 2017, 46, 3134-3184.

[7] a) L. Oar-Arteta, T. Wezendonk, X. Sun, F. Kapteijn, J. Gascon, Materials Chemistry Frontiers 2017, 1, 1709-1745; b) V. P. Santos, T. A. Wezendonk, J. J. D. Jaén, A. I. Dugulan, M. A. Nasalevich, H.-U. Islam, A. Chojecki, S. Sartipi, X. Sun, A. A. Hakeem, A. C. J. Koeken, M. Ruitenbeek, T. Davidian, G. R. Meima, G. Sankar, F. Kapteijn, M. Makkee, J. Gascon, Nature Communications 2015, 6, 6451; c) X. Sun, A. I. Olivos-Suarez, L. Oar-Arteta, E. Rozhko, D. Osadchii, A. Bavykina, F. Kapteijn, J. Gascon, ChemCatChem 2017, 9, 1854-1862; d) X. Sun, A. I. O. Suarez, M. Meijerink, T. van Deelen, S. Ould-Chikh, J. Zečević, K. P. de Jong, F. Kapteijn, J. Gascon, Nature Communications 2017, 8, 1680.

[8] X. Sun, A. I. Olivos-Suarez, D. Osadchii, M. J. V. Romero, F. Kapteijn, J. Gascon, Journal of Catalysis 2018, 357, 20-28.

[9] W. Xia, A. Mahmood, R. Q. Zou, Q. Xu, Energ Environ Sci 2015, 8, 1837-1866.

[10] R. Kortlever, J. Shen, K. J. Schouten, F. Calle-Vallejo, M. T. Koper, The journal of physical chemistry letters 2015, 6, 4073-4082.

[11] a) Q. Lu, F. Jiao, Nano Energy 2016, 29, 439-456; b) H. R. Jhong, S. C. Ma, P. J. A. Kenis, Current Opinion in Chemical Engineering 2013, 2, 191-199; c) J.-P. Jones, G. K. S. Prakash, G. A. Olah, Israel Journal of Chemistry 2014, 54, 1451-1466; d) X. Lu, Y. Wu, X. Yuan, L. Huang, Z. Wu, J. Xuan, Y. Wang, H. Wang, ACS Energy Letters 2018, 3, 2527-2532; e) X. Liu, J. Xiao, H. Peng, X. Hong, K. Chan, J. K. Nørskov, Nature Communications 2017, 8, 15438.

[11] a) S. Gonen, L. Elbaz, Current Opinion in Electrochemistry 2018, 9, 179-188; b) C. Kim, F. Dionigi, V. Beermann, X. Wang, T. Moller, P. Strasser, Adv Mater 2018, e1805617; c) Y. Kim, A. Jo, Y. Ha, Y. Lee, D. Lee, Y. Lee, C. Lee, Electroanalysis 2018, 30, 2861-2868.

[13] B. Mondal, P. Sen, A. Rana, D. Saha, P. Das, A. Dey, ACS Catalysis 2019, 9, 3895-3899.

[14] A. V. Rudnev, Y. C. Fu, I. Gjuroski, F. Stricker, J. Furrer, N. Kovacs, S. Vesztergom, P. Broekmann, Chemphyschem 2017, 18, 3153-3162.

[15] L. Han, W. Zhou, C. Xiang, ACS Energy Letters 2018, 3, 855-860.

[16] M. Rumayor, A. Dominguez-Ramos, A. Irabien, Sustainable Production and Consumption 2019, 18, 72-82.

[17] Y. Hori, H. Konishi, T. Futamura, A. Murata, O. Koga, H. Sakurai, K. Oguma, Electrochimica Acta 2005, 50, 5354-5369.

[18] a) H. Won da, H. Shin, J. Koh, J. Chung, H. S. Lee, H. Kim, S. I. Woo, Angew Chem Int Ed Engl 2016, 55, 9297-9300; b) M. Ma, K. Liu, J. Shen, R. Kas, W. A. Smith, ACS Energy Lett 2018, 3, 1301-1306; cH. Zhang, Y. Ma, F. J. Quan, J. J. Huang, F. L. Jia, L. Z. Zhang, Electrochemistry Communications 2014, 46, 63-66.

[19] Y. Zhai, L. Chiachiarelli, N. Sridhar, ECS Transactions 2009, 19, 1-13.

[20] a) Q. Lu, J. Rosen, F. Jiao, Chemcatchem 2015, 7, 38-47; b) J. F. He, A. X. Huang, N. J. J. Jobnson, K. E. Dettelbach, D. M. Weekes, Y. Cao, C. P. Berlinguette, Inorganic Chemistry 2018, 57, 14624-14631.

[21] R. Hinogami, S. Yotsuhashi, M. Deguchi, Y. Zenitani, H. Hashiba, Y. Yamada, Ecs Electrochemistry Letters 2012, 1, H17-H19.

[22] R. S. Kumar, S. S. Kumar, M. A. Kulandainathan, Electrochemistry Communications 2012, 25, 70-73.

[23] Y. L. Wang, P. F. Hou, Z. Wang, P. Kang, Chemphyschem 2017, 18, 3142-3147.

[24] X. L. Jiang, H. B. Li, J. P. Xiao, D. F. Gao, R. Si, F. Yang, Y. S. Li, G. X. Wang, X. H. Bao, Nano Energy 2018, 52, 345-350.

[25] J. Albo, D. Vallejo, G. Beobide, O. Castillo, P. Castano, A. Irabien, ChemSusChem 2017, 10, 1100-1109.

[26] S. Dou, J. J. Song, S. B. Xi, Y. H. Du, J. Wang, Z. F. Huang, Z. C. J. Xu, X. Wang, Angew Chem Int Edit 2019, 58, 4041-4045.

[27] L. Ye, J. Liu, Y. Gao, C. Gong, M. Addicoat, T. Heine, C. Wöll, L. Sun, Journal of Materials Chemistry A 2016, 4, 15320-15326.

[28] X. Kang, Q. Zhu, X. Sun, J. Hu, J. Zhang, Z. Liu, B. Han, Chem Sci 2016, 7, 266-273.

[29] I. Hod, M. D. Sampson, P. Deria, C. P. Kubiak, O. K. Farha, J. T. Hupp, Acs Catalysis 2015, 5, 6302-6309.

[30] B.-X. Dong, S.-L. Qian, F.-Y. Bu, Y.-C. Wu, L.-G. Feng, Y.-L. Teng, W.-L. Liu, Z.-W. Li, ACS Applied Energy Materials 2018, 1, 4662-4669.

[31] J. X. Wu, S. Z. Hou, X. D. Zhang, M. Xu, H. F. Yang, P. S. Cao, Z. Y. Gu, Chemical Science 2019, 10, 2199-2205.

[32] N. Kornienko, Y. Zhao, C. S. Kley, C. Zhu, D. Kim, S. Lin, C. J. Chang, O. M. Yaghi, P. Yang, J Am Chem Soc 2015, 137, 14129-14135.

[33] X. L. Jiang, H. H. Wu, S. J. Chang, R. Si, S. Miao, W. X. Huang, Y. H. Li, G. X. Wang, X. H. Bao, Journal of Materials Chemistry A 2017, 5, 19371-19377.
[34] C. W. Kung, C. O. Audu, A. W. Peters, H. Noh, O. K. Farha, J. T. Hupp, Acs Energy Letters 2017, 2, 2394-2401.
[35] X. Y. Tan, C. Yu, C. T. Zhao, H. W. Huang, X. C. Yao, X. T. Han, W. Guo, S. Cui, H. L. Huang, J. S. Qiu, Acs Applied Materials & Interfaces 2019, 11, 9904-9910.
[36] K. Zhao, Y. M. Liu, X. Quan, S. Chen, H. T. Yu, Acs Applied Materials & Interfaces 2017, 9, 5302-5311.
[37] M. K. Kim, H. J. Kim, H. Lim, Y. Kwon, H. M. Jeong, Electrochimica Acta 2019, 306, 28-34.
[38] Y. F. Ye, F. Cai, H. B. Li, H. H. Wu, G. X. Wang, Y. S. Li, S. Miao, S. H. Xie, R. Si, J. Wang, X. H. Bao, Nano Energy 2017, 38, 281-289.
[39] C. M. Zhao, X. Y. Dai, T. Yao, W. X. Chen, X. Q. Wang, J. Wang, J. Yang, S. Q. Wei, Y. E. Wu, Y. D. Li, Journal of the American Chemical Society 2017, 139, 8078-8081.
[40] F. P. Pan, H. G. Zhang, K. X. Liu, D. Cullen, K. More, M. Y. Wang, Z. X. Feng, G. F. Wang, G. Wu, Y. Li, Acs Catalysis 2018, 8, 3116-3122.
[41] D. H. Nam, O. S. Bushuyev, J. Li, P. De Luna, A. Seifitokaldani, C. T. Dinh, F. P. G. de Arquer, Y. H. Wang, Z. Q. Liang, A. H. Proppe, C. S. Tan, P. Todorovic, O. Shekhah, C. M. Gabardo, J. W. Jo, J. M. Choi, M. J. Choi, S. W. Baek, J. Kim, D. Sinton, S. O. Kelley, M. Eddaoudi, E. H. Sargent, Journal of the American Chemical Society 2018, 140, 11378-11386.
[42] X. Q. Wang, Z. Chen, X. Y. Zhao, T. Yao, W. X. Chen, R. You, C. M. Zhao, G. Wu, J. Wang, W. X. Huang, J. L. Yang, X. Hong, S. Q. Wei, Y. Wu, Y. D. Li, Angew Chem Int Edit 2018, 57, 1944-1948.
[43] W. W. Guo, X. F. Sun, C. J. Chen, D. X. Yang, L. Lu, Y. D. Yang, B. X. Han, Green Chemistry 2019, 21, 503-508.
[44] R. Wang, X. Sun, S. Ould-Chikh, D. Osadchii, F. Bai, F. Kapteijn, J. Gascon, ACS Applied Materials & Interfaces 2018, 10, 14751-14758.
[45] Y. Zheng, P. Cheng, J. Xu, J. Han, D. Wang, C. Hao, H. R. Alanagh, C. Long, X. Shi, Z. Tang, Nanoscale 2019, 11, 4911-4917.
[46] Y. Guo, H. J. Yang, X. Zhou, K. L. Liu, C. Zhang, Z. Y. Zhou, C. Wang, W. B. Lin, Journal of Materials Chemistry A 2017, 5, 24867-24873.
[47] a) Z. Weng, J. Jiang, Y. Wu, Z. Wu, X. Guo, K. L. Materna, W. Liu, V. S. Batista, G. W. Brudvig, H. Wang, J Am Chem Soc 2016, 138, 8076-8079; b) G. Zhu, Y. Li, H. Zhu, H. Su, S. H. Chan, Q. Sun, ACS Catalysis 2016, 6, 6294-6301; cS. Lin, C. S. Diercks, Y.-B. Zhang, N. Kornienko, E. M. Nichols, Y. Zhao, A. R. Paris, D. Kim, P. Yang, O. M. Yaghi, C. J. Chang, Science 2015, 349, 1208-1213.
[48] X. M. Hu, M. H. Ronne, S. U. Pedersen, T. Skrydstrup, K. Daasbjerg, Angew Chem Int Ed Engl 2017, 56, 6468-6472.
[49] W. W. Kramer, C. C. L. McCrory, Chemical Science 2016, 7, 2506-2515.
[50] F. Schuth, M. D. Ward, J. M. Buriak, Chemistry of Materials 2018, 30, 3599-3600.
[51] Lide, David R., ed. CRC handbook of chemistry and physics. Vol. 85. CRC press, 2004.
[52] B. Liu, H. Shioyama, T. Akita, Q. Xu, J Am Chem Soc 2008, 130, 5390-5391.
[53] a) R. Walczak, B. Kurpil, A. Savateev, T. Heil, J. Schmidt, Q. Qin, M. Antonietti, M. Oschatz, Angew Chem Int Edit 2018, 57, 10765-10770; b) M. Antonietti, M. Oschatz, Advanced Materials 2018, 30.
[54] A. Ramirez, L. Gevers, A. Bavykina, S. Ould-Chikh, J. Gascon, ACS Catalysis 2018, 8, 9174-9182.
[55] T. Burdyny, W. A. Smith, Energ Environ Sci 2019.

Entry for the Table of Contents

FOCUS REVIEW

Engineering Metal-organic frameworks to prepare catalysts for the electrochemical reduction of CO_2

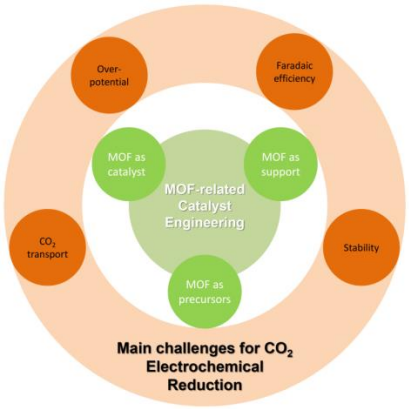

*Riming Wang, Freek Kapteijn, Jorge Gascon**

Page No. – Page No.

Engineering Metal-Organic Frameworks for the Electrochemical Reduction of CO_2: A Mini-review